Research Paper

Creating Functional Vesicle Assemblies from Vesicles and Nanoparticles

Robert J. Mart,[1] Kwan Ping Liem,[1] and Simon J. Webb[1,2]

Abstract. Vesicles (liposomes) have been shown to be excellent vehicles for drug delivery, yet assemblies of vesicles (vesicle aggregates) have been used infrequently in this context. However vesicle assemblies have useful properties not available to individual vesicles; their size can cause localisation in specific tissues and they can incorporate more functionality than is possible with individual vesicles. This article reviews progress on controlling the properties of vesicle assemblies *in vitro*, applications of vesicle assemblies *in vivo*, and our recent creation of magnetic nanoparticle–vesicle assemblies. The latter assemblies contain vesicles crosslinked by coated Fe_3O_4 nanoparticles and this inclusion of magnetic functionality makes them magnetically responsive, potentially allowing magnetically-induced contents release. This article describes further studies on the *in vitro* formation of these magnetic nanoparticle–vesicle assemblies, including the effect of changing magnetic nanoparticle concentration, pH, adhesive lipid structure and bilayer composition. These investigations have led to the development of thermally-sensitive magnetic nanoparticle–vesicle assemblies that release encapsulated methotrexate on warming.

KEY WORDS: aggregation; liposome; magnetic nanoparticle; magnetically responsive; magnetoliposome.

INTRODUCTION

Vesicles (liposomes) have proved to be invaluable in pharmaceutical and biological chemical research because they have cell membrane-mimetic surfaces and they can act as carriers for both hydrophilic and hydrophobic pharmaceuticals (1). Their biomimetic surface can either be engineered to mimic a cell surface by adding artificial lipids, or masked by adding PEG-lipids that prevent recognition and clearance from the body *via* the reticuloendothelial system (RES). The first approach can generate vesicles that target their drug payload to particular cell types, e.g. immunoliposomes (1), whilst masking with PEG lipids creates "stealth liposomes", where the PEG layer prevents interactions with biomolecules and inhibits recognition by phagocytes (2).

Within the enormous body of research on vesicles, the vast majority has used individual vesicles for biomimetic studies or as pharmaceutical carriers. However, recently there has been increasing interest in creating assemblies of vesicles as mimics of cell–cell adhesion and as drug delivery vehicles that can target particular organs *in vivo*. The creation of these vesicle assemblies requires multivalent ligands to cross-link the vesicles into networks. Indeed the study of vesicle aggregation by multivalent ligands has improved understanding of cellular agglomeration by biological multivalent ligands like antibodies or lectins, and may lead to the formation of "artificial tissue". Vesicle assemblies can have distinct properties that depend upon the type of multivalent ligand employed as cross-linker; polymers/proteins, other vesicles and nanoparticles have all been used (Fig. 1). The extensive body of work on vesicle aggregation can be conveniently reviewed according to these categories, with current and potential *in vivo* applications of each vesicle assembly type discussed.

(a) Vesicle cross-linking by polymers and proteins

Vesicle aggregation by proteins or polymers mimics the binding of these multivalent ligands to cells and has been intensively investigated. This focus is in recognition of its biological importance; many important cellular processes, such as signal transduction and the immune response, rely upon intramembrane receptor aggregation or intermembrane cell agglomeration by multivalent ligands (Fig. 1). In particular, what determines the balance between cross-linking cells and multivalent binding to a single cell surface is not well understood. This is an important research area as cooperative binding of a multivalent ligand to receptors on a single cell surface underpins the development of high avidity drugs (3), while the alternative binding mode, the crosslinking of cells by multivalent ligands, has been suggested as a new mechanism for biological intervention by multivalent drugs. The latter approach mimics the way that IgM forms large conglomerates of antigens that are easily opsonised by macrophages; indeed the use of multivalent ligands to form "cancer nets" around tumours and retard tumour growth has been suggested (4). Similarly, it has been suggested that the aggregation of other pathogens by synthetic multivalent polymers could form particles that are easier for the body to clear (5).

[1] Manchester Interdisciplinary Biocentre and the School of Chemistry, University of Manchester, 131 Princess St, Manchester, M1 7DN, UK.
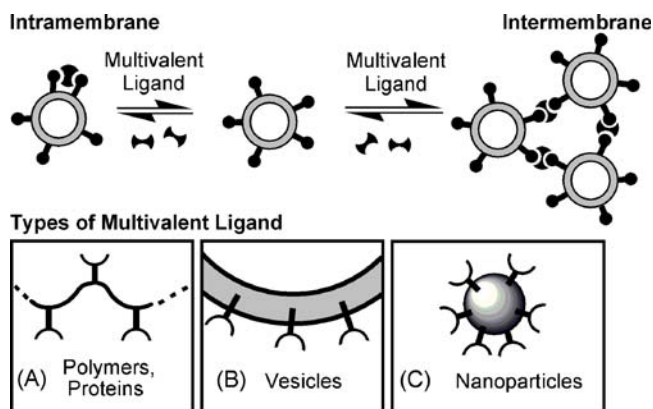[2] To whom correspondence should be addressed. (e-mail: S.Webb@ manchester.ac.uk)

Fig. 1. Vesicle aggregation by multivalent ligands. **a** Polymers, proteins. **b** Vesicles. **c** Nanoparticles.

Fig. 2. Localisation of vesicles in the lymph nodes by *in vivo* formation of vesicle aggregates.

A variety of different interactions, mediated through macromolecules like proteins, peptides, DNA and dendrimers, have been used to cross-link vesicles. In particular, the strength and selectivity of the biotin-avidin pairing has made its use ubiquitous in biomolecular science and this linkage was one of the first to be used to form vesicle aggregates (6). In pioneering work, Zasadzinski *et al.* showed avidin or streptavidin would aggregate phospholipid vesicles (100 nm diameter) that contained between 0.03% and 0.24% mol/mol of biotin-capped lipid in their membranes, with the most extensive aggregation at biotin:avidin ratios below 0.4:1. Similarly, Vermette *et al.* found the ratio of DSPE-PEG-biotin lipid to avidin determined the size of aggregates, with the largest aggregates (10 μm diameter) forming when vesicles containing 0.2% mol/mol biotin-lipid were mixed with 0.5 equivalents of biotin (7). This increase in size caused by avidin-mediated aggregation has led to novel ways of targeting vesicles to organs. In ground-breaking work, Ogihara-Umeda *et al.* used aggregation to clear 100 nm diameter vesicles containing ^{67}Ga-deferoxamine (8) or ^{111}In-deferoxamine from the blood (9). Vesicles of this size are accumulated by tumours, but a significant fraction remains in the bloodstream. Labelling the vesicles with 0.3% mol/mol biotinylated distearoyl phosphatidylethanolamine (biotin-DSPE) allowed subsequent intravenous injection of avidin or neutravidin to give vesicle aggregates in the bloodstream, which were more easily recognised and removed by the RES to leave behind vesicles located within the tumours. Avidin-mediated vesicle aggregation has also been used by Phillips and co-workers, who showed in 2000 that the formation of vesicle aggregates by avidin can give increased delivery of ^{99m}Tc to the lymph nodes (10). Subcutaneous injection of 136 nm diameter vesicles labelled with 1% mol/mol biotin-DSPE and containing a ^{99m}Tc radio-label was followed by subcutaneous injection of avidin at a nearby site. Both components drained into the lymphatic system, where they mixed to form large vesicle aggregates that became trapped in the next lymph node encountered (Fig. 2). An eightfold increase in vesicle retention in the popliteal nodes and iliac nodes was noted, and the vesicle aggregates formed could selectively deliver ^{99m}Tc and patent blue violet dye to sentinel lymph nodes. Furthermore, varying the injection site allowed the vesicle aggregates to be targeted to the abdominal and mediastinal lymph nodes (11,12). As
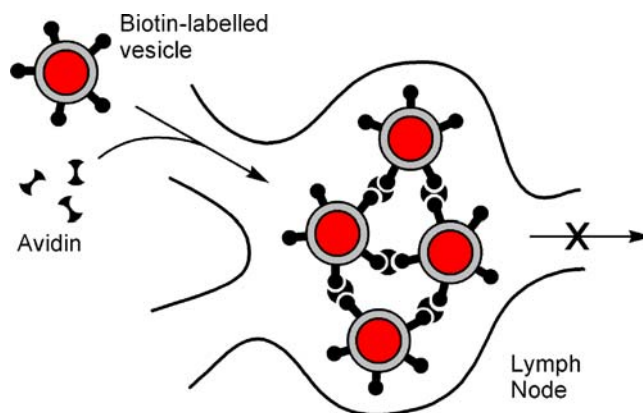
expected, labelling avidin with ^{111}In revealed co-localisation of the avidin and biotin-vesicles within the mediastinal lymph nodes after intrapleural or intraperitoneal injection. The size of these aggregates *in vivo* was not determined and could only be inferred from *in vitro* studies, which showed significant aggregation at avidin:biotin ratios as low as 0.04:1 (13).

Few other cross-linking interactions have been developed to create vesicle aggregates *in vivo*, despite the wide variety used to cross-link vesicles *in vitro* (14). A notable example was recently reported by Moghimi and co-workers, who used IgM to cross-link subcutaneously injected immuno-PEG liposomes. These immuno-PEG liposomes, which incorporated both mPEG$_{350}$-lipids (10% mol/mol) and IgG-capped PEG$_{1000}$ lipids (1% mol/mol) showed no interaction with non-specific IgM. However, injection of anti-IgG IgM gave an up to twofold increase in the retention of these vesicles in regional lymph nodes, presumably through the formation of large vesicle aggregates in the lymphatic system (15).

Moghimi *et al.* suggested peptide- or protein-lipids as alternative recognition elements to IgG-capped PEG$_{1000}$ lipids, yet polypeptides themselves have been widely used *in vitro* as cross-linking multivalent ligands. Paleos and co-workers have conducted extensive studies on the formation of vesicle aggregates and have produced large vesicle aggregates by mixing phosphate-lipid doped vesicles with guanidylated dendrimers (16) or polyarginine (17). Very large aggregates (>1000 nm diameter) resulted from the addition of
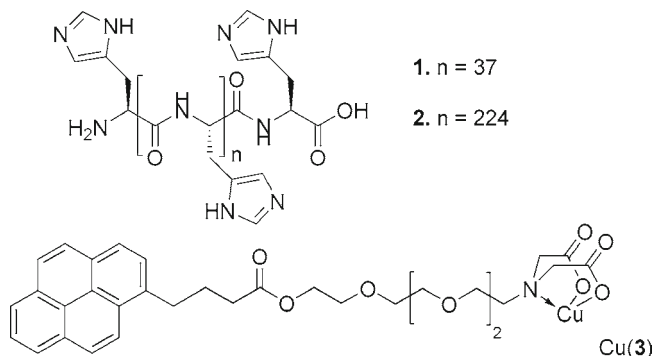

1. n = 37

2. n = 224

Fig. 3. Vesicles containing adhesive lipid Cu(**3**) can be aggregated by polyhistidines **1** and **2**.

polyarginine to vesicles (100 nm diameter) bearing 5% mol/mol di(hexadecyl)phosphate, but heating to the bilayer melting temperature (T_m) resulted in partial penetration of the polypeptide into the bilayer. Similarly, guanidylated dendrimers often caused vesicles to fuse rather than aggregate, or form multicompartment "vesosomes" (18). To prevent unwanted vesicle fusion we used the histidine-Cu (iminodiacetate) (His-Cu(IDA)) interaction (Fig. 3), which is extensively used for affinity chromatography and is a weaker interaction than the guanidinium-phosphate link (19). Distearoyl phosphatidylcholine (DSPC) vesicles (800 nm diameter) containing 5% mol/mol of a fluorescent Cu(IDA)-capped lipid Cu(**3**), ([Cu(**3**)-DSPC] vesicles) were agglomerated by the addition of polyhistidine **1**, but not by acetyl histidine. The size of the vesicle aggregates could be increased by using longer polyhistidine (**2**) since there is a decrease in vesicle-vesicle repulsion for this longer cross-linker. However, isothermal titration calorimetry revealed that aggregate stability did not increase concomitantly with increases in aggregate size or increases in ligand valency. Instead, the surface density of adhesive lipid Cu(**3**) should determine if binding to the vesicle surface is intra- or intermembrane (Fig. 1); in general low surface densities of adhesive lipids will favour the formation of vesicle aggregates. These studies also showed control over bilayer composition is crucial for controlling the balance between adhesion and fusion in vesicle aggregates. Although aggregates composed of [Cu(**3**)-DSPC] vesicles or [Cu(**3**)-DMPC/chol] vesicles (bilayers composed of 1:1 dimyristoyl phosphatidylcholine:cholesterol) appeared to be stable over several days, egg yolk phosphatidylcholine (EYPC) vesicles containing Cu(**3**) quickly fused upon the addition of **1** to give large unilamellar vesicles. This fusogenic character is due to the unsaturated phospholipids in EYPC, which stabilise the highly negatively curved regions present in the "stalk" that forms between vesicles prior to fusion (20).

(b) Vesicle cross-linking by other vesicles

Vesicles doped with adhesive lipids are themselves multivalent ligands, and can provide AB-type mixed vesicle aggregates (Fig. 4a). Mixing populations of vesicles that bear complementary adhesive lipids is of great interest, in part due to the similarity of this process to cell–cell recognition in tissue and cell-natural carrier recognition during the binding of lipoproteins. These AB-type vesicle assemblies also have orthogonal storage capacity that allows incompatible reagents to be stored within the different vesicle sub-populations; for example prodrugs released from adhering vesicles could mix to form a pharmacologically active species. Examples of mixed vesicle assemblies include vesicles linked through

guanidinium-phosphate salt bridges, charge–charge interactions and barbiturate-triaminopyrimidine hydrogen bonds (21–23). Multivalent recognition between vesicles (Fig. 4a) appears to be weaker than recognition between polymers and vesicle surfaces (Fig. 4b), which may reflect a lower degree of organisation in a dynamic multivalent display (on a vesicle surface) compared to a covalently-linked multivalent display (a polymer). Much like polymer-mediated vesicle adhesion, both aggregation and fusion are possible outcomes, but careful control of membrane composition can give stable vesicle assemblies.

Biomimetic studies such as these can illuminate the physical basis of cell–cell and cell–vesicle adhesion, and the latter has particularly relevance for targeted drug delivery (24). In cells, the adhesion molecules (CAMs) cluster together into focal adhesion complexes during cell–cell recognition, and this preorganisation is believed to strengthen intercellular links. To verify that this CAM clustering enhanced adhesion we developed fluorinated Cu(IDA)-capped lipid Cu(**4**) (Fig. 5), which can phase separate from fluid phospholipid bilayers. The pyrene-perfluoroalkyl membrane anchor in Cu(**4**) drives the adhesive lipid to phase separate into "sticky patches" in solid-ordered (DSPC at 25°C) or liquid-ordered phospholipid bilayers (DMPC/chol). However, in liquid disordered bilayers, like DMPC at 25°C, Cu(**4**) mixes with the bilayer and disperses evenly over the vesicle surface (25). Thus adjusting membrane composition can "switch on" or "switch off" lipid phase separation, which in turn should modulate the strength of vesicle-vesicle links. Indeed no vesicle aggregation resulted when [Cu(**4**)-DMPC] vesicles, which have Cu(**4**) dispersed evenly over the surface, were mixed with DMPC/chol vesicles containing 5% mol/mol histidine-capped lipid **5** ([**5**-DMPC/chol] vesicles). However, when [**5**-DMPC/chol] vesicles were mixed with [Cu(**4**)-DMPC/chol] vesicles, which have "sticky patches" of Cu(**4**), large vesicle aggregates (>20 μm in diameter) that contained both types of vesicle were observed (Fig. 6) (26). Using phase separation to induce vesicle agglomeration is also an attractive prospect for future *in vivo* drug delivery applications, for example enzymatically-induced phase separation of an adhesive lipid could lead to the formation of vesicle aggregates in targeted tissues.

(c) Vesicle Cross-Linking by Nanoparticles

Combining nanoparticles with vesicles (themselves nano-sized objects) is a key part of the developing field of nanomedicine (27). These nanoparticles are usually included within individual vesicles (28, 29), so the use of nanoparticles as cross-linking multivalent ligands was an intriguing prospect; it was recently reported that carboxy-functionalised polystyrene nanoparticles actually inhibited the aggregation of biotin-doped dilauroylphosphatidylcholine vesicles by streptavidin (30). Using magnetic nanoparticles (MNPs) in this context is particularly interesting given the explosion of research into the biological and pharmaceutical applications of MNPs; they have been applied as contrast agents for magnetic resonance imaging, as hyperthermia agents and as magnetically-directed drug delivery vehicles (31). Interestingly, both magnetic nanoparticles and vesicle aggregates have been used to target the lymph nodes; intravenously injected dextran-coated magnetic nanoparticles (ferumoxtran-10) are
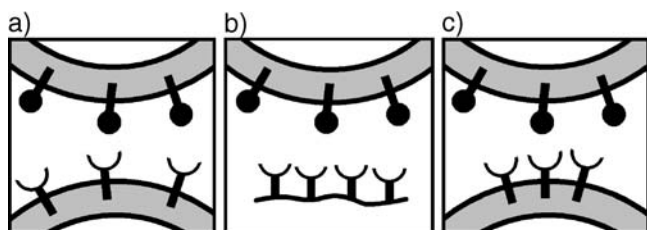

Fig. 4. Multivalent vesicle binding to **a** another vesicle; **b** polymer/protein; **c** another vesicle with pre-organised patches of adhesive lipid.
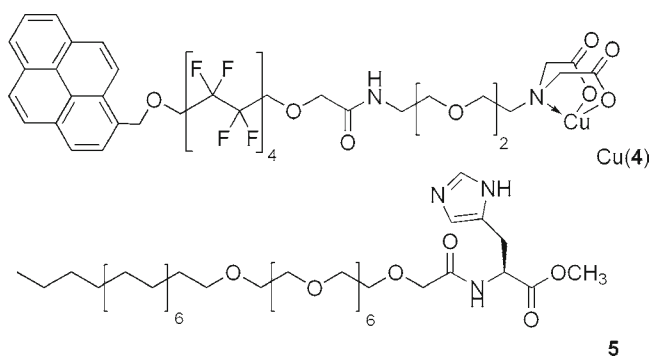
Fig. 5. Phase-separating adhesive lipid Cu(**4**) and conjugate partner, histidine-capped lipid **5**.

used for metastatic lymph node imaging as these 30 nm diameter nanoparticles accumulate in non-cancerous lymphatic tissue (32).

Magnetic nanoparticles had already been combined with individual phospholipid vesicles, either as encapsulated ferrofluids (33,34) or membrane-embedded magnetite nanoparticles (35). These "magnetoliposomes" have drug delivery applications, with the magnetic nanoparticles providing extra functionality that allows magnetic targeting of the vesicles (36,37) or controlled contents release *via* magnetic hyperthermia (35). The latter application uses the magnetic nanoparticles as nano-sized heaters to heat the phospholipid bilayer beyond its melting temperature (T_m); the resulting liquid disordered bilayers are highly permeable and encapsulated species can escape. For example, large unilamellar dipalmitoyl phosphatidylcholine (DPPC) vesicles encapsulating doxorubicin and with magnetite nanoparticles (8 nm diameter) in their membranes completely released the encapsulated drug upon exposure to an alternating magnetic field (frequency 3.5 MHz, induction 1.5 mT). The magnetic heating was very selective for the vesicle membranes and there was little warming of the bulk solution.

Rather than placing magnetic nanoparticles in the bilayer membrane or in the encapsulated volume of vesicles, we decided to use the surface of coated magnetic nanoparticles as multivalent ligands to cross-link vesicles into functionalised vesicle assemblies. Magnetic targeting should allow these vesicle-magnetic nanoparticle assemblies to be formed in or relocated to specific regions of the body, where their large size may slow clearance. Subsequent exposure to an alternating magnetic field could selectively release the contents of the vesicle-magnetic nanoparticle assemblies without affecting the surrounding tissue (Fig. 7).
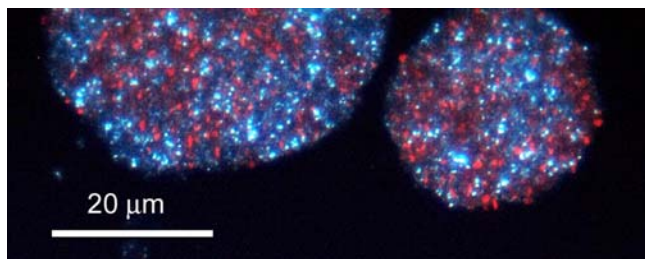

Fig. 6. Fluorescence micrograph of vesicle aggregates composed of vesicles containing 5% mol/mol lipid **5** in DMPC/chol (labelled with rhodamine) adhering to vesicles containing 5% mol/mol Cu(**4**) (which fluoresce blue) in DMPC/chol.
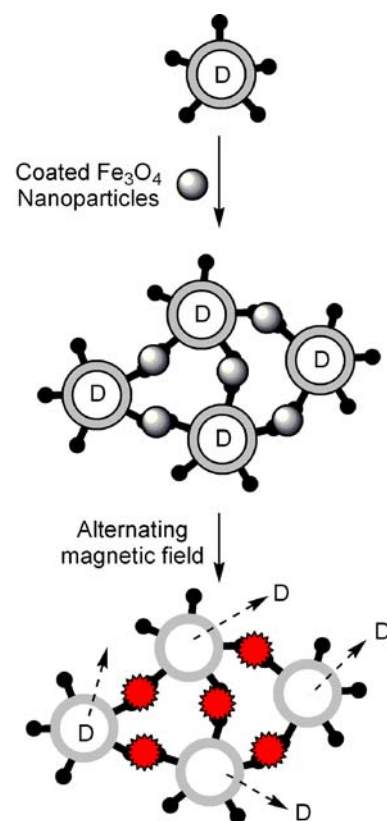

Fig. 7. Formation of magnetic nanoparticle–vesicle assemblies (MNPs), and potential use as magnetically triggerable drug delivery vehicles.

Given our success creating stable mixed vesicle aggregates with [Cu(**4**)-DMPC/chol] vesicles (26), these were chosen as the vesicle component of our magnetic nanoparticle–vesicle assemblies. To create the corresponding multivalent histidine ligand from Fe_3O_4 nanoparticles, dopamine-histidine conjugate **6** was synthesised. Catechol groups anchor tightly to Fe_3O_4 surfaces, so mixing **6** with hydrothermally synthesised magnetite nanoparticles (10 nm diameter) gave coated nanoparticles [**6**-MNP] with 90±10% of the surface coated with histidine groups (Fig. 8).

Fluorescence microscopy and scanning electron microscopy showed mixing [**6**-MNP] nanoparticles with [Cu(**4**)-DMPC/chol] vesicles at pH 5.4 gave large networks of cross-linked vesicle-nanoparticle assemblies (38). Encapsulation studies with sulforhodamine B showed the nanoparticles did not disrupt the integrity of the vesicle membranes, and the vesicles in the assemblies retained encapsulated substances. The resulting vesicle assemblies could be magnetically manipulated by a
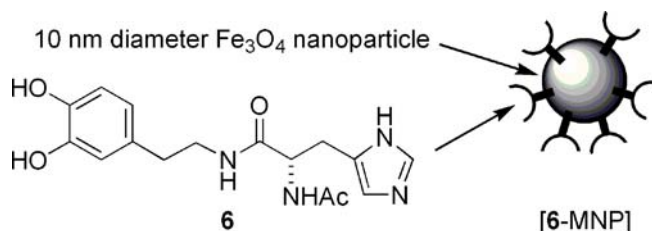

Fig. 8. Histidine–dopamine conjugate **6** and a coated magnetic nanoparticle [**6**-MNP].

5,350 G neodymium iron boron magnet (Fig. 9); nanoparticle–vesicle assemblies can be magnetically extracted from a mixture containing non-magnetic vesicles, whilst different populations of magnetic nanoparticle–vesicle assemblies could be sequentially manipulated by orthogonal magnetic fields to create patterns of vesicles on surfaces or within micro-flow cells.

The next challenge was to explore the scope of this methodology, and described herein are recent studies into the effect of changing pH, nanoparticle concentration and adhesive lipid structure on the formation of these magnetic nanoparticle–vesicle assemblies. These studies culminate with the development of magnetically manipulable vesicle-nanoparticle conjugates that released encapsulated drugs and biomolecules upon warming to a set triggering temperature.

MATERIALS AND METHODS

Chemicals, including compounds **1** and **2**, were used as received from Sigma-Aldrich. A N48 neodymium iron boron magnet, magnetic field 5350 G, was purchased from e-magnets UK, Sheffield S2 5QT, U.K. Compounds H$_2$**3** (11-bis(carboxymethyl)amino-3,6,9-trioxaundecyl 4-(pyren-1-yl)butanoate), H$_2$**4** (8-(bis(carboxymethyl)amino)-3,6-dioxaoctyl (2,2,3,3,4,4,5,5,6,6,7,7,8,8,9,9-hexadecafluoro-10-(pyren-1-ylmethoxy)decyloxy)acetamide), **5** and **6** were synthesized as detailed previously (19,26,38), and gave satisfactory spectroscopic and analytical data. UV-Visible spectra were recorded on a Cary 400 Scan UV spectrophotometer or a Jasco V-660 spectrophotometer. Fluorescence spectra were recorded on a Perkin-Elmer LS55 luminescence spectrometer. Images of vesicles and vesicle-nanoparticle aggregates were captured using a Zeiss Axio Imager A1 fluorescence microscope fitted with a Canon Powershot G6 digital camera.

General Procedure for the Preparation of Vesicles by Extrusion. Unilamellar [H$_2$**3**-DMPC/chol] or [H$_2$**4**-DMPC/chol] vesicles (800 nm diameter) had a membrane composition of 47.5% mol/mol dimyristoyl phosphatidylcholine (DMPC), 47.5% mol/mol cholesterol (chol) and 5% mol/mol of either H$_2$**3** or H$_2$**4**. Unilamellar [H$_2$**4**-DMPC/DPPC] vesicles (800 nm diameter) had a membrane composition of 9.5% mol/mol DMPC, 85.5% mol/mol DPPC and 5% mol/mol H$_2$**4**. Vesicles of all compositions were prepared for vesicle-nanoparticle aggregation studies in a similar manner to previously published procedures (26,38). The required amounts of lipids (20 μmol) and either H$_2$**3** or H$_2$**4** (1.05 mL of a 1 mM solution of H$_2$**3** or H$_2$**4** in chloroform) were

Fig. 9. Fluorescence micrograph showing magnetic sedimentation of rhodamine-labelled magnetic nanoparticle–vesicle aggregates (*in suspension, right*) into a compressed layer of vesicle assemblies (*left*).

dissolved in spectroscopic grade ethanol-free chloroform (5 mL), then the solvent removed under reduced pressure to leave a lipid thin-film on the interior wall of a round-bottomed flask. The appropriate buffer (either MES buffer: 20 mM MES, 100 mM NaCl, pH 5.4 at 25°C, 1 mL, or MOPS buffer: 20 mM MOPS, 100 mM NaCl, pH 7.2 at 25°C, 1 mL) was added to the flask and the contents vortex mixed to detach the thin film. This suspension of multilamellar vesicles was passed 19 times through an 800 nm polycarbonate membrane in an Avestin Liposofast extrusion apparatus, to give a suspension of unilamellar vesicles (1 mL). All vesicle suspensions were freshly prepared prior to mixing with magnetic nanoparticles.

General Procedure for the Preparation of Vesicles by Interdigitation-Fusion. A mixture of 9.5% mol/mol DMPC, 85.5% mol/mol DPPC and 5% mol/mol of H$_2$**4** were dissolved in chloroform in a small round-bottomed flask and the solvent evaporated under reduced pressure to yield a thin lipid film. The film was hydrated in the appropriate buffer solution containing the compound to be encapsulated, using mixing on a rotary evaporator (at atmospheric pressure) with the water bath set at 50°C (10°C above the transition temperature of the lipid mixture). The resulting suspension was then sonicated in a heated ultrasonic bath until the suspension appeared transparent. Absolute ethanol (0.05 mL) was added and the mixture allowed to cool, giving an opaque, viscous, interdigitated phase. The flask was then placed in a water bath at 50°C and a stream of nitrogen passed over the solution until the ethanol was removed (approx 10–20 min).

Synthesis of Coated Fe$_3$O$_4$ Magnetic Nanoparticles [6-MNP]. (*Nanoparticles were coated following a modification to a literature procedure*) (38): To surface-functionalise magnetite nanoparticles, compound **6** (7.2 mg, 21.6 μmol) was dissolved in methanol (2 mL), followed by addition of magnetite nanoparticles (30 mg, 129.6 μmol) whilst the solution was sonicated. The particles were sonicated under nitrogen for 6 hours. Application of a 5 kG permanent magnet for 5 min sedimented the particles and the resulting clear supernatant solution was removed. The sediment was re-dispersed by sonication and washed with methanol as above (3×10 mL) to remove unreacted **6**. The coated particles were re-suspended in methanol (10 mL) and the solvent removed under vacuum. Further drying under high vacuum gave the coated nanoparticles (30 mg, ~90%) as a black, fine powder (yield based on 80–100% coating efficiency) (38).

General Procedure for the Preparation of Nanoparticle–Vesicle Aggregates. Copper(II) chloride solution in MES or MOPS buffer (2 μL, 50 mM, 0.1 μmol) was added to a suspension of [H$_2$**3**-DMPC/chol], [H$_2$**4**-DMPC/chol] or [H$_2$**4**-DMPC/DPPC] vesicles (1 mL, 2 mM lipids, [H$_2$**3**] or [H$_2$**4**]= 0.1 mM, 0.1 μmol) with gentle mixing to give [Cu(**3**)-DMPC/chol], [Cu(**4**)-DMPC/chol] or [Cu(**4**)-DMPC/DPPC] vesicles. Dry [**6**-MNP] nanoparticles (1.2 mg) were dispersed in distilled water (1 mL) by sonication to give a stock suspension of [**6**-MNP] (1.2 mg/mL). Vesicle-nanoparticle aggregates were prepared by gently mixing the suspension of [**6**-MNP] in distilled water (0 to 200 μL) with [Cu(**3**)-DMPC/chol], [Cu(**4**)-DMPC/chol] or [Cu(**4**)-DMPC/DPPC] vesicles (1 mL, concentration of Cu(**3**) or Cu(**4**)=0.1 mM) at a 1:1 ratio of **6** to Cu(**3**)/Cu(**4**). The mixture was then left to aggregate for one minute, then the aggregates sedimented with a perma-
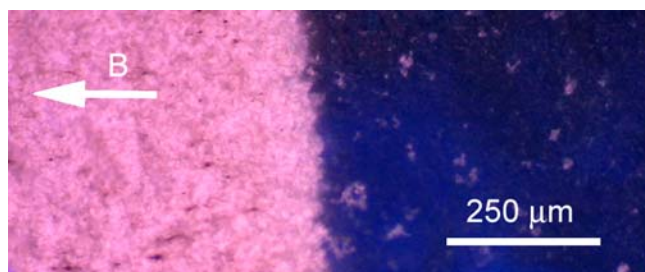
nent magnet. Enough of the clear supernatant was removed to return the aggregate solution to its initial lipid concentration and volume (2 mM lipids, 1 mL), then the sedimented aggregates redispersed by gentle vortex mixing.

Fluorescence Microscopy Imaging of Vesicle-Nanoparticle Aggregates. Vesicle aggregates were observed on glass slides, from samples of aggregate suspensions with a 2 mM lipid concentration.

Encapsulation of Cytochrome C, 5/6-Carboxyfluorescein, Methotrexate or FITC-Dextran in vesicles

Purification by GPC. The vesicle solution (1 mL) was diluted to 2.5 mL with additional buffer of the appropriate type and loaded onto a pre-equilibrated PD-10 Sephadex desalting column. The vesicle solution was then eluted using a further 3.5 mL of buffer.

Purification by Magnetic Sedimentation. Vesicle suspensions were placed upon a 5-kG magnet until a compact vesicle plug had formed at the bottom of the vial and the supernatant solution was visually free of turbidity. As much of the supernatant was removed as possible without disturbing the vesicle plug (typically 60% of the initial volume), and replaced with the equal volume of the appropriate buffer solution. Briefly vortex mixing of the vial regenerated the vesicle suspension. This procedure was repeated at least 6 times and until the concentration of unencapsulated material was <0.1% of the initial concentration.

Release of Encapsulated Dyes from Nanoparticle/Vesicle Aggregates. Fluorescence or UV-visible spectroscopic analysis followed immediately after GPC/magnetic purification; for each measurement an aliquot was dissolved in MOPS buffer (2 mL) in a fluorescence or spectrophotometric cuvette to give a total lipid concentration of 0.01 mM. At the end of each run, Triton X-100 (4 μL, 25% *v/v*) was added with shaking to release all of the encapsulated material and provide the maximum fluorescence/absorbance values (100% release of encapsulated material).

RESULTS AND DISCUSSION

The Role of Adhesive Lipid Phase Separation in the Formation Vesicle-Nanoparticle Aggregates

The crucial role that lipid phase separation plays in enhancing vesicle aggregation was clear from our previous studies (26); histidine-labelled [5-DMPC/chol] vesicles could adhere to [Cu(4)-DMPC/chol] vesicles but not [Cu(3)-DMPC/chol] vesicles. In contrast, polyhistidine could efficiently aggregate these [Cu(3)-DMPC/chol] vesicles (without phase-separation of adhesive lipids). Given that Fe_3O_4 magnetic nanoparticles coated with compound 6 ([6-MNP]) are self-assembled multivalent ligands, it was not clear whether these coated magnetic nanoparticles would behave like a covalently linked multivalent display (e.g. polyhistidine) or like a non-covalent multivalent display of individual ligands (e.g. phase-separated Cu(4) in DMPC/chol vesicles). Therefore to determine the adhesive characteristics of

[6-MNP], [Cu(3)-DMPC/chol] vesicles (without phase-separated islands of adhesive lipid) were mixed with [6-MNP]; if magnetic nanoparticle–vesicle assemblies result then the comparison of [6-MNP] with polyhistidine would be more accurate. Vesicles containing 5% mol/mol of Cu(3) in DMPC/chol vesicles at pH 5.4 (20 mM MES buffer, 100 mM NaCl) were produced in an identical manner as previously (26). Mixing these vesicles containing Cu(3) with coated magnetic nanoparticles [6-MNP] at pH 5.4 gave the increase in turbidity that suggested formation of vesicle aggregates. Indeed when the turbid suspension was visualised by fluorescence microscopy, large vesicle aggregates were observed, although these aggregates (up to 20 μm diameter) were smaller than those observed when DMPC/chol vesicles containing phase separated adhesive lipid Cu(4) were mixed with [6-MNP] nanoparticles (aggregates from 20 to 100 μm diameter) (Fig. 10). As observed with assemblies containing Cu(4) (38), magnetic nanoparticle–vesicle assemblies containing Cu(3) were responsive to external magnetic fields. Application of a 5,350 G N48 neodymium iron boron permanent magnet to the base of a cuvette containing these magnetic nanoparticle–vesicle assemblies resulted in rapid sedimentation, whilst sedimentation took over 12 h in the absence of a magnetic field. Magnetic sedimentation was prevented by the addition of one equivalent of EDTA (Fig. 11a), which extracted the copper(II) and dissociated the assemblies.

Comparing the magnetic response of vesicle assemblies containing Cu(3) to vesicle assemblies containing phase-separated lipid Cu(4) showed only a small difference in sedimentation rate (Fig. 11a). However, varying the concentration of [6-MNP] showed more clearly the differences between the two adhesive lipids. Although nanoparticle–vesicle assemblies containing Cu(3) still formed at pH 5.4 when lower concentrations of coated magnetic nanoparticles were used, they were smaller (3–10 μm diameter at 30 μg/mL 6-MNP, 3–8 μm diameter at 10 μg/mL 6-MNP) than assemblies containing Cu(4). A threefold decrease in the concentration of magnetic nanoparticles (to 30 μg/mL) before mixing with [Cu(3)-DMPC/chol] vesicles slowed the magnetic sedimentation rate more than fivefold and the vesicle-nanoparticle suspension in the cuvette remained turbid after 25 min. In comparison, [Cu(4)-DMPC/
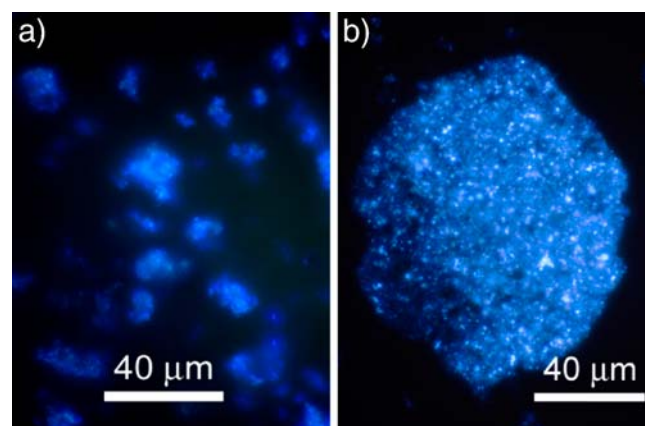

Fig. 10. Fluorescence micrographs of magnetic nanoparticle–vesicle aggregates formed by mixing [6-MNP] nanoparticles with **a** [Cu(3)-DMPC/chol] vesicles at pH 5.4 or **b** [Cu(4)-DMPC/chol] vesicles at pH 5.4.

chol] vesicles with phase-separated lipid Cu(**4**) gave larger aggregates when mixed with these lower concentrations of coated magnetic nanoparticles [**6**-MNP], and the resulting aggregates were correspondingly more responsive to applied external magnetic fields (Fig. 11b).

Increasing the pH to 7.2 revealed an even greater difference in the binding of [Cu(**3**)-DMPC/chol] vesicles and [Cu(**4**)-DMPC/chol] vesicles to [**6**-MNP]. Vesicles containing 5% mol/mol Cu(**4**) in DMPC/chol were able to form nanoparticle–vesicle aggregates when mixed with [**6**-MNP] at pH 7.2, although at 10 to 20 μm in diameter they were smaller than vesicle assemblies formed at pH 5.4. However [Cu(**3**)-DMPC/chol] vesicles formed only very small aggregates when mixed with [**6**-MNP] at pH 7.2 (<3 μm diameter) and application of the 5 kG permanent magnet sedimented only the magnetic nanoparticles, leaving the [Cu(**3**)-DMPC/chol] vesicles in suspension. Since an increase in pH should decrease the fraction of histidine residues that are protonated

and strengthen binding between [**6**-MNP] and membrane-embedded copper(iminodiacetate) lipids, weaker binding at higher solution pHs suggests adhesion may be enhanced by the electrostatic attraction of [**6**-MNP]$^{n+}$ to the surface of the phospholipid vesicles, which carry a slight negative charge (39).

These observations suggest that, as previously observed, the phase separation of these Cu(IDA)-capped adhesive lipids does cause a corresponding increase in the strength of multivalent binding; in this case to the multiple histidines exposed on the surface of [**6**-MNP] nanoparticles. Nonetheless, under favourable conditions, such as high concentrations of histidine-coated Fe_3O_4 nanoparticles at pH 5.4, it was possible to form magnetically responsive vesicle-nanoparticle assemblies using adhesive lipids that are dispersed evenly over the vesicle surfaces. Given many phase-separating synthetic lipids must be chemically synthesised prior to use, these observations imply that non-phase separating but commercially available adhesive lipids should also give magnetic nanoparticle–vesicle assemblies.
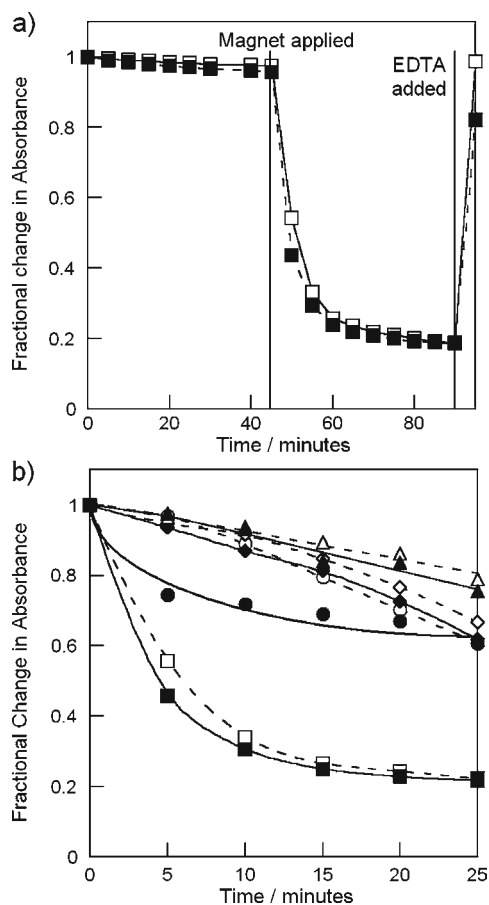
Magnetic Purification of Magnetic Nanoparticle–Vesicle Assemblies

Although [Cu(**4**)-DMPC/chol] vesicles at pH 5.4 can retain encapsulated dyes during the formation of vesicle-nanoparticle assemblies, dye retention had yet to be proved at physiological pH. This also gave an opportunity to show one of the key advantages of incorporating magnetic functionality into these vesicle assemblies. In an external magnetic field the assemblies can be magnetically sedimented into a plug and the supernatant containing the unencapsulated material removed, which allows (non-magnetic) species that are difficult to remove by standard methods such as dialysis or gel permeation chromatography (GPC) to be separated from the vesicles. [Cu(**4**)-DMPC/chol] vesicles were produced by extrusion of the lipid mixture in a solution of cytochrome c (20 μM) in MOPS buffer, at pH 7.2. Horse heart cytochrome c is an intensely coloured red protein (ε=106,000 $M^{-1}cm^{-1}$ at 410 nm) with a molecular weight of 12 kDa. Due to its high molecular weight, it was not possible to separate unencapsulated cytochrome c from [Cu(**4**)-DMPC/chol] vesicles, as both fractions eluted from the GPC PD-10 column as a single red band. Therefore histidine-coated magnetic [**6**-NMP] nanoparticles were added to the [Cu(**4**)-DMPC/chol] vesicles in cytochrome c solution, resulting in the immediate formation of vesicle-nanoparticle aggregates. Subsequent application of the 5 kG magnet sedimented the vesicle-nanoparticles aggregates into a plug at the base of the vial, allowing the red supernatant to be removed by decantation (1.5 mL of the 2.5 mL total). A fresh volume of buffer (1.5 mL) was added and the vesicle-nanoparticle aggregates re-suspended by gentle agitation. A further six iterations of sedimentation-decantation eventually gave a suspension of vesicle-nanoparticle aggregates with net concentration of cytochrome c=0.4 μM, which upon sedimentation gave a colourless supernatant containing <0.1 μM cytochrome c. The encapsulated volume was calculated as 2%, in line with encapsulation volumes typical for 800 nm diameter vesicles. Furthermore, unlike GPC, there was no dilution of the sample. The same technique can be used to separate small molecules that can be difficult to remove from some vesicle preparations, such as methotrexate (Fig. 12).

Fig. 11. a Change in turbidity with time of suspensions containing [**6**-MNP] mixed with either [Cu(**3**)-DMPC/chol] vesicles (*empty squares*) or [Cu(**4**)-DMPC/chol] vesicles (*filled squares*) at pH 5.4; an external 5 kG magnetic field was applied at 45 min and EDTA was added at 90 min. **b** Change in turbidity after application of a 5 kG magnetic field to mixtures of [Cu(**3**)-DMPC/chol] vesicles (*empty symbols*) or [Cu(**4**)-DMPC/chol] vesicles (*filled symbols*) with different concentrations of [**6**-MNP]; 100 μg/mL (*empty squares, filled squares*), 30 μg/mL (*empty circles, filled circles*), 10 μg/mL (*empty diamonds, filled diamonds*), 5 μg/mL (*empty triangles, filled triangles*). All *curve fits* are to guide the eye.
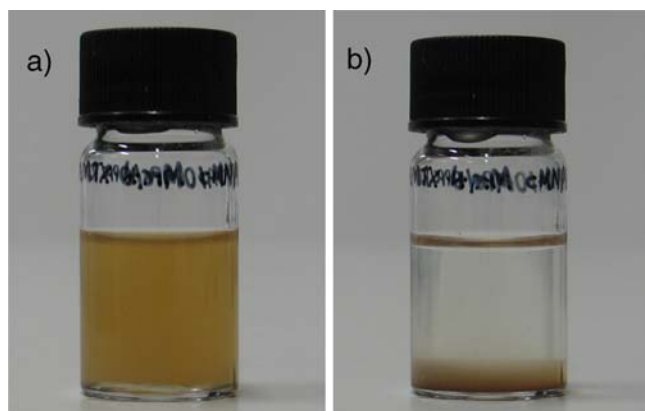
Fig. 12. **a** A suspension of [Cu(**4**)-DPPC/DMPC]/[**6**-MNP] magnetic nanoparticle–vesicle aggregates containing methotrexate. **b** Application of 5 kDa magnet sediments the magnetic nanoparticle–vesicle aggregates to form a plug.

THERMALLY SENSITIVE VESICLE-NANOPARTICLE AGGREGATES

Light- (40,41), oxidation- (42) and pH- (1,43) triggered release of vesicle contents have been shown to be efficient methods for the release of encapsulated substances, but recently reported magnetically-triggered release is of particular interest. Magnetic hyperthermia of magnetic nanoparticles is used to melt the bilayers of thermally-sensitive vesicles, resulting in the total release of encapsulated substances. The DMPC/chol vesicles used previously could not be used for magnetic hyperthermia as the presence of cholesterol keeps the bilayer in the liquid-ordered phase and prevents the bilayer from melting. To apply magnetic hyperthermia to magnetic nanoparticle–vesicle assemblies, the vesicle bilayers must be in the solid-ordered phase (gel phase) and have a melting temperature that is easily accessible, such as mixtures of DMPC and DPPC that melt in the range of 30°C to 42°C (44). Since the application of magnetic vesicle-nanoparticle assemblies *in vivo* would require the solution pH to be ~7, only vesicles containing phase separated adhesive lipid Cu(**4**) can be used, since Cu(**3**) cannot form vesicle assemblies at this pH. Fortunately, the pyrene-perfluoroalkyl motif found in the membrane anchor of Cu(**4**) is known to phase-separate from gel-phase DSPC bilayers (26), suggesting that Cu(**4**) would also phase separate from DMPC/DPPC bilayers below their T_m. This combination of thermal sensitivity and adhesive lipid clustering suggested [Cu(**4**)-DPPC/DMPC]/[**6**-MNP] vesicle-nanoparticle assemblies would be the optimal platform for drug delivery systems *in vivo*.

Bilayers composed of 1:10 DMPC:DPPC were described as possessing a melting temperature of 37°C (45), which is ideal for cell culture applications. Changing the membrane composition to pure DPPC also gives access to vesicle-nanoparticle assemblies that would be stable at body temperature with drug release triggered by gentle warming to 42°C. Vesicles containing 5% mol/mol Cu(**4**) in 1:10 DMPC:DPPC were synthesised by extrusion above 40°C in MOPS buffer (20 mM MOPS, 100 mM NaCl, pH 7.2), before being allowed to cool to 25°C. To assess the extent to which Cu(**4**) phase separated from these DMPC:DPPC bilayers, the ratio of

pyrene excimer fluorescence at 480 nm (E) to monomer fluorescence at 377 nm (M) was determined after excitation at 346 nm (25). Extensive phase separation is indicated by an E/M ratio greater than 0.4, e.g. [Cu(**4**)-DMPC/chol] vesicles have an E/M ratio ~0.4 at pH 7.2 and 25°C. In comparison, [Cu(**4**)-DMPC/DPPC] vesicles had an E/M ratio of 0.66 at pH 7.2 and 25°C, confirming that Cu(**4**) extensively phase-separated from gel-phase DMPC:DPPC membranes and should form vesicle-magnetic nanoparticle assemblies at pH 7.2. Gratifyingly, when these [Cu(**4**)-DMPC/DPPC] vesicles (1 mL) were mixed with [**6**-MNP] nanoparticles (100 μg in 0.1 mL) at pH 7.2, large magnetically responsive vesicle assemblies were observed by fluorescence microscopy.

For initial studies, three standard payloads were selected for thermally triggered release from vesicle-nanoparticle assemblies; 5/6-carboxyfluorescein (5/6-CF), the potent anti-cancer drug methotrexate (MTX) and a fluorescently-tagged polysaccharide (4 kDa FITC-dextran). The alleviation of self-quenching caused by 5/6-CF release allows easy determination of release efficiency, while MTX is a non-fluorescent drug with a similar size. The polysaccharide FITC-dextran is much larger and should show much slower release rates than 5/6-CF and MTX; it serves as a model for small proteins and low molecular weight heparin. [Cu(**4**)-DMPC/DPPC] vesicles containing encapsulated 5/6-carboxyfluorescein (internal concentration=0.5 mM) were produced by extrusion at 40°C, then cooled to 25° and the nonencapsulated dye removed by standard GPC methodology. Subsequent addition of [**6**-MNP] nanoparticles produced vesicle aggregates as expected, albeit with some visible leakage of the encapsulated dye. This was readily removed by magnetic sedimentation and supernatant exchange since GPC proved to be less effective on these large assemblies. These magnetic nanoparticle–vesicle assemblies displayed reduced membrane integrity compared to those formed at pH 5.4; fluorescence spectroscopy revealing 6% leakage of 5/6-CF over 1 h, compared to only 0.3% leakage over four hours from non-aggregated DMPC/DPPC vesicles. However, upon heating to 40°C, there was rapid and complete release of the encapsulated dye within 10 min (Fig. 13a).

Similarly, [Cu(**4**)-DMPC/DPPC] vesicles containing encapsulated methotrexate (produced by interdigitation/fusion (45), 27.5 mM internal concentration) also formed stable vesicle-nanoparticle aggregates when mixed with [**6**-MNP] nanoparticles. These assemblies were also very stable at 20°C, but upon heating to 40°C rapid release of the yellow encapsulated methotrexate was observed; 70% release at 40°C when measured at 50 min. The presence of the magnetic nanoparticles in these assemblies also simplified the quantification of the release of non-fluorescent methotrexate; the turbid suspension was cleared by the application of an external magnetic field to leave behind a transparent supernatant containing released methotrexate, which could be directly analysed by spectrophotometry (Fig. 12).

The release of 4 kDa FITC-dextran was used as a model for other biomacromolecules, such as enzymes and glycosaminoglycans. FITC-dextran encapsulating [Cu(**4**)-DMPC/DPPC] vesicles (internal concentration=8 mM) were once again produced by interdigitation/fusion, but in this case it was not possible to separate the macromolecule from the [Cu(**4**)-DMPC/DPPC] vesicles by GPC. Therefore, the same
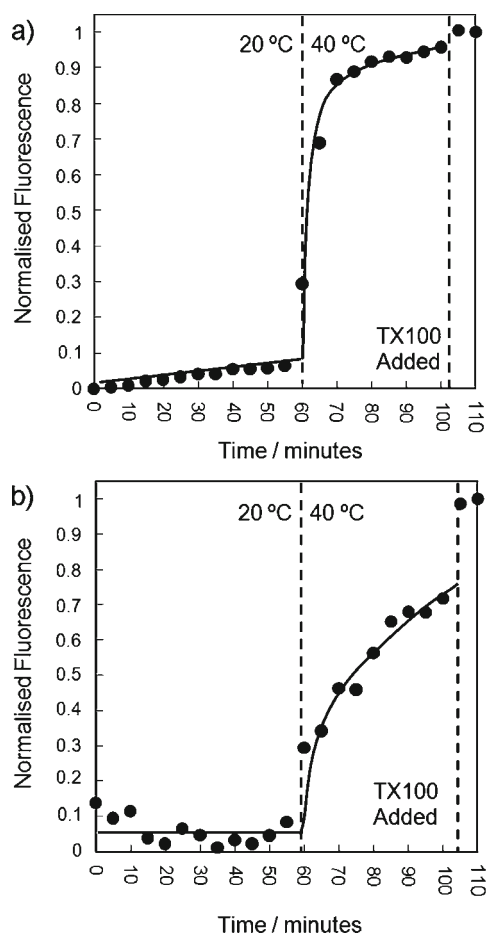
Fig. 13. a Release of encapsulated species from [Cu(**4**)-DPPC/DMPC]/[**6**-MNP] magnetic nanoparticle–vesicle aggregates; **a** 5/6-carboxyfluorescein. **b** 4 kDa FITC-dextran.

iterative sequence of magnetic sedimentation, decantation and dilution used with the cytochrome c-containing vesicles was used to remove non-encapsulated FTC-dextran. The resulting purified aggregates did not measurably release FITC-dextran at 20°C, but on heating to 40°C there was rapid release of the encapsulated macromolecule. This release occurred at a slower rate than for the smaller 5/6-CF dye (Fig. 13b) and reflects the difficulty in transporting large polar molecules across membranes, even when the membranes are in the liquid-disordered phase. Nonetheless, these vesicle assemblies have the potential to release most categories of pharmaceutical agents in response to a thermal signal, which in future we hope will be provided by magnetic hyperthermia.

CONCLUSIONS

Given the rapid development of vesicles as drug delivery vehicles, the application of vesicle assemblies in pharmaceutical research is an under-investigated area. Current applications have relied on the change in size caused by vesicle aggregation to locate vesicles in particular regions of the body. However, this methodology does not exploit assembly formation to its fullest extent, as the assembly process allows

additional functionality to be included; for example a cross-linking multivalent polymer could be biologically active or labelled with a biologically active species. Alternatively nanoparticles can be used; these can have an enormous range of properties that includes fluorescent, magnetic and catalytic functionality. Furthermore, heterogenous vesicle assemblies composed of different types of vesicle can encapsulate mutually incompatible species that only mix upon release from the vesicles in the assembly. Given the large body of work in the chemical literature on the formation of vesicle assemblies and aggregates, there is a clear opportunity to apply this knowledge in the development of new drug delivery platforms.

Magnetic nanoparticle–vesicle assemblies are a particularly interesting class of functionalised vesicle assemblies, as these have the potential for magnetically-induced drug release and magnetic targeting to particular tissues. We have described the formation of assemblies that link together magnetite nanoparticles and phospholipid vesicles, showed them to be magnetically responsive, and showed they can store drugs or biopolymers. The formation of these assemblies can be controlled by adjusting the pH and magnetite nanoparticle concentration, with low pHs and high nanoparticle concentrations increasing the size of the assemblies formed. Phase separation of the adhesive lipid in the vesicle bilayers strengthens binding of the vesicles to the nanoparticles and is particularly noticeable at higher pHs, but phase separation is not necessarily required for the formation of magnetic nanoparticle–vesicle assemblies. Changing the composition of the vesicles provided thermally-sensitive magnetic nanoparticle–vesicle assemblies that released their contents upon warming to 40°C. The *in vivo* creation of these magnetic nanoparticle–vesicle aggregates could lead to new imaging applications and/or magnetically induced delivery of encapsulated species to targeted organs.

We hope that this methodology for the creation of magnetic nanoparticle–vesicle assemblies will facilitate research in this area and lead to medical applications. Studies are ongoing into the use of magnetic nanoparticle–vesicle arrays as cell culture scaffolds and magnetically induced drug release from thermally sensitive vesicle assemblies.

ACKNOWLEDGEMENTS

REFERENCES

1. Torchilin VP. Recent advances with liposomes as pharmaceutical carriers. Nat Rev Drug Discov 2005;4:145–60. doi:10.1038/nrd1632.
2. Levchenko TS, Rammohan R, Lukyanov AN, Whiteman KR, Torchilin VP. Liposome clearance in mice: the effect of a separate and combined presence of surface charge and polymer coating. Int J Pharm 2002;240:95–102. doi:10.1016/S0378-5173(02)00129-1.
3. Kiessling LL, Gestwicki JE, Strong LE. Synthetic multivalent ligands in the exploration of cell–surface interactions. Curr Opin Chem Biol 2000;4:696–703. doi:10.1016/S1367-5931(00)00153-8.
4. Menger FM, Bian J, Sizova E, Martinson DE, Seredyuk VA. Bolaforms with fourteen galactose units: a proposed site-directed cohesion of cancer cells. Org Lett 2004;6:261–4. doi:10.1021/ol030135k.

5. Gestwicki JE, Strong LE, Cairo CW, Boehm FJ, Kiessling LL. Cell aggregation by scaffolded receptor clusters. Chem Biol 2002;9:163–9. doi:10.1016/S1074-5521(02)00102-3.

6. Chiruvolu S, Walker S, Israelachvili J, Schmitt FJ, Leckband D, Zasadzinski JA. Higher order self-assembly of vesicles by site-specific binding. Science 1994;264:1753–6. doi:10.1126/science.8209255.

7. Vermette P, Taylor S, Dunstan D, Meagher L. Control over PEGylated-liposome aggregation by neutravidin-biotin interactions investigated by photon correlation spectroscopy. Langmuir 2002;18:505–11. doi:10.1021/la0109967.

8. Ogihara-Umeda I, Sasaki T, Nishigori H. Active removal of radioactivity in the blood circulation using biotin-bearing liposomes and avidin for rapid tumour imaging. Eur J Nucl Med 1993;20:170–2. doi:10.1007/BF00168879.

9. Ogihara-Umeda I, Sasaki T, Toyama H, Oda K, Senda M, Nishigori H. Rapid tumor imaging by active background reduction using biotin-bearing liposomes and avidin. Cancer Res 1994;54:463–7.

10. Phillips WT, Klipper R, Goins B. Novel method of greatly enhanced delivery of liposomes to lymph nodes. J Pharmacol Exp Ther 2000;295:309–13.

11. Phillips WT, Medina LA, Klipper R, Goins B. A novel approach for the increased delivery of pharmaceutical agents to peritoneum and associated lymph nodes. J Pharmacol Exp Ther 2002;303:11–6. doi:10.1124/jpet.102.037119.

12. Medina LA, Calixto SM, Klipper R, Phillips WT, Goins B. Avidin/biotin–liposome system injected in the pleural space for drug delivery to mediastinal lymph nodes. J Pharm Sci 2004;93:2595–608. doi:10.1002/jps.20163.

13. Fung VWH, Chiu GNC, Mayer LD. Application of purging biotinylated liposomes from plasma to elucidate influx and efflux processes associated with accumulation of liposomes in solid tumors. Biochim Biophys Acta 2003;1611:63–9. doi:10.1016/S0005-2736(02)00704-6.

14. Paleos CM, Sideratou Z, Tsiourvas D. Molecular recognition of complementary liposomes in modeling cell - cell recognition. ChemBioChem 2001;2:305–10. doi:10.1002/1439-7633(20010504)2:5<305::AID-CBIC305>3.0.CO;2-9.

15. Moghimi SM, Moghimi M. Enhanced lymph node retention of subcutaneously injected IgG1-PEG$_{2000}$-liposomes through pentameric IgM antibody-mediated vesicular aggregation. Biochim Biophys Acta 2008;1778:51–5. doi:10.1016/j.bbamem.2007.08.033.

16. Sideratou Z, Foundis J, Tsiourvas D, Nezis IP, Papadimas G, Paleos CM. A novel dendrimeric "glue" for adhesion of phosphatidyl choline-based liposomes. Langmuir 2002;18:5036–9. doi:10.1021/la020150i.

17. Tsogas I, Tsiourvas D, Nounesis G, Paleos CM. Interaction of poly-L-arginine with dihexadecyl phosphate/phosphatidylcholine liposomes. Langmuir 2005;21:5997–6001. doi:10.1021/la050475+.

18. Pantos A, Tsogas I, Paleos CM. Guanidinium group: a versatile moiety inducing transport and multicompartmentalization in complementary membranes. BBA Biomembranes 2008;1778:11–23. doi:10.1016/j.bbamem.2007.12.003.

19. Wang X, Mart RJ, Webb SJ. Vesicle aggregation by multivalent ligands: relating crosslinking ability to surface affinity. Org Biomol Chem 2007;5:2498–505. doi:10.1039/b706662g.

20. Webb SJ, Trembleau L, Mart RJ, Wang X. Membrane composition determines the fate of aggregated vesicles. Org Biomol Chem 2005;3:3615–7. doi:10.1039/b510647h.

21. Marchi-Artzner V, Gulik-Krzywicki T, Guedeau-Boudeville M-A, Gosse C, Sanderson JM, Dedieu J-C, Lehn J-M. Selective adhesion, lipid exchange and membrane-fusion processes between vesicles of various sizes bearing complementary molecular recognition groups. ChemPhysChem 2001;2:367–76. doi:10.1002/1439-7641(20010618)2:6<367::AID-CPHC367>3.0.CO;2-#.

22. Menger FM, Seredyuk VA. Internally catalyzed separation of adhered lipid membranes. J Am Chem Soc 2003;125:11800–1. doi:10.1021/ja030334z.

23. Sideratou Z, Tsiourvas D, Paleos CM. Molecular recognition of complementary liposomes: the enhancing role of cholesterol. Langmuir 2000;16:9186–91. doi:10.1021/la000166d.

24. Barragan V, Menger FM, Caran KL, Vidil C, Morere A, Montero J-L. A mannose-6-phosphonate-cholesterylamine conjugate as a specific molecular adhesive linking cancer cells with vesicles. Chem Commun 2001. 85–6. doi:10.1039/b008446h.

25. Webb SJ, Greenaway K, Bayati M, Trembleau L. Lipid fluorination enables phase separation from fluid phospholipid bilayers. Org Biomol Chem 2006;4:2399–407. doi:10.1039/b603373n.

26. Mart RJ, Liem KP, Wang X, Webb SJ. The effect of receptor clustering on vesicle–vesicle adhesion. J Am Chem Soc 2006;128:14462–3. doi:10.1021/ja0657612.

27. Ferrari M. Cancer nanotechnology: opportunities and challenges. Nat Rev Cancer 2005;5:161–71. doi:10.1038/nrc1566.

28. Wu G, Mikhailovsky A, Khant HA, Fu C, Chiu W, Zasadzinski JA. Remotely triggered liposome release by near-infrared light absorption via hollow gold nanoshells. J Am Chem Soc 2008;130:8175–7. doi:10.1021/ja802656d.

29. Dif A, Henry E, Artzner F, Baudy-Floc'h M, Schmutz M, Dahan M, Marchi-Artzner V. Interaction between water-soluble peptidic CdSe/ZnS nanocrystals and membranes: formation of hybrid vesicles and condensed lamellar phases. J Am Chem Soc 2008;130:8289–96. doi:10.1021/ja711378g.

30. Zhang L, Dammann K, Baeb SC, Granick S. Ligand–receptor binding on nanoparticle-stabilized liposome surfaces. Soft Matter 2007;3:551–3. doi:10.1039/b618172d.

31. Arruebo M, Fernández-Pacheco F, Ibarra MR, Santamaría J. Magnetic nanoparticles for drug delivery. Nanotoday 2007;2:22–32.

32. Corot C, Robert P, Idée J-M, Port M. Recent advances in iron oxide nanocrystal technology for medical imaging. Adv Drug Deliver Rev 2006;58:1471–504. doi:10.1016/j.addr.2006.09.013.

33. Sabaté R, Barnadas-Rodríguez R, Callejas-Fernández J, Hidalgo-Álvarez R, Estelrich J. Preparation and characterization of extruded magnetoliposomes. Int J Pharm 2008;347:156–62. doi:10.1016/j.ijpharm.2007.06.047.

34. Wijaya A, Hamad-Schifferli K. High-density encapsulation of Fe$_3$O$_4$ nanoparticles in lipid vesicles. Langmuir 2007;23:9546–50. doi:10.1021/la701128b.

35. Babincová M, Čičmanec P, Altanerová V, Altaner Č, Babinec P. AC-magnetic field controlled drug release from magnetoliposomes: design of a method for site-specific chemotherapy. Bioelectrochem 2002;55:17–9. doi:10.1016/S1567-5394(01)00171-2.

36. Dandamudi S, Campbell RB. The drug loading, cytotoxicity and tumor vascular targeting characteristics of magnetite in magnetic drug targeting. Biomaterials 2007;28:4673–83. doi:10.1016/j.biomaterials.2007.07.024.

37. Babincová M, Altanerová V, Lambert M, Altaner Č, Šramka M, Machová E, Babinec P. Site specific in vivo targeting of magnetoliposomes in external magnetic field. Z Naturforsch 2000;55c:278–81.

38. Liem KP, Mart RJ, Webb SJ. Magnetic assembly and patterning of vesicle/nanoparticle aggregates. J Am Chem Soc 2007;129:12080–1. doi:10.1021/ja075000e.

39. Alonso JM, Llácer C, Vila AO, Figueruelo JE, Molina FJ. Effect of the osmotic conditions on the value of ζ potential of DMPC multilamellar liposomes. Colloids Surfaces A: Physicochem Eng Aspects 1995;95:11–4. doi:10.1016/0927-7757(94)02994-4.

40. Zhang Z-Y, Shum P, Yates M, Messersmith PB, Thompson DH. Formation of fibrinogen-based hydrogels using phototriggerable diplasmalogen liposomes. Bioconj Chem 2002;13:640–6. doi:10.1021/bc015580j.

41. Shum P, Kim J-M, Thompson DH. Phototriggering of liposomal drug delivery systems. Adv Drug Deliv Rev 2001;53:273–84. doi:10.1016/S0169-409X(01)00232-0.

42. Napoli A, Valentini M, Tirelli N, Müller M, Hubbell JA. Oxidation-responsive polymeric vesicles. Nat Mater 2004;3:183–9. doi:10.1038/nmat1081.

43. Lomas H, Canton I, MacNeil S, Du J, Armes SP, Ryan AJ, Lewis AL, Battaglia G. Biomimetic pH sensitive polymersomes for efficient DNA encapsulation and delivery. Adv Mater 2007;19:4238–43. doi:10.1002/adma.200700941.

44. Messersmith PB, Starke S. Thermally triggered calcium phosphate formation from calcium-loaded liposomes. Chem Mater 1998;10:117–24. doi:10.1021/cm9702528.

45. Messersmith PB, Vallabhanei S, Nguyen V. Preparation of calcium-loaded liposomes and their use in calcium phosphate formation. Chem Mater 1998;10:109–16. doi:10.1021/cm970251f.